THE JOURNAL OF BIOLOGICAL CHEMISTRY VOL. 287, NO. 29, pp. 24092–24102, July 13, 2012

Leukemia Inhibitory Factor Coordinates the Down-regulation of the Visual Cycle in the Retina and Retinal-pigmented Epithelium*[S]

Received for publication, May 4, 2012 Published, JBC Papers in Press, May 29, 2012, DOI 10.1074/jbc.M112.378240

Ana J. Chucair-Elliott[‡§], Michael H. Elliott[‡], Jiangang Wang[¶], Gennadiy P. Moiseyev[‖], Jian-Xing Ma[**], Luis E. Politi[§], Nora P. Rotstein[§], Shizuo Akira[‡‡], Satoshi Uematsu[‡‡], and John D. Ash[¶1]**

*From the Department of [‡]Ophthalmology, [‖]Medicine, and **Physiology, University of Oklahoma Health Sciences Center, Oklahoma City, Oklahoma 73104, [§]Instituto de Investigaciones Bioquímicas de Bahía Blanca-Departamento de Biología, Bioquímica y Farmacia, Universidad Nacional del Sur, Bahía Blanca 8000, Argentina, [‡‡]Laboratory of Host Defense, World Premier International Immunology Frontier Research Center Osaka University, Osaka 565-0871, Japan, and the [¶]Department of Ophthalmology, University of Florida, Gainesville, Florida 32610*

Background: Neurocytokines (LIF and CNTF) mediate photoreceptor protection and down-regulation of phototransduction.
Results: LIF down-regulates the visual cycle decreasing RPE65 expression and activity through activation of STAT3 in RPE.
Conclusion: The gp130/STAT3 pathway is independently modulated in RPE and retina for coordinated control of visual cycle activity.
Significance: A single, endogenous paracrine factor (LIF) can stimulate RPE cells to reduce production of 11-*cis*-retinal.

Leukemia inhibitory factor (LIF), an interleukin-6 family neurocytokine, is up-regulated in response to different types of retinal stress and has neuroprotective activity through activation of the gp130 receptor/STAT3 pathway. We observed that LIF induces rapid, robust, and sustained activation of STAT3 in both the retina and retinal pigmented epithelium (RPE). Here, we tested whether LIF-induced STAT3 activation within the RPE can down-regulate RPE65, the central enzyme in the visual cycle that provides the 11-*cis*-retinal chromophore to photoreceptors *in vivo*. We generated conditional knock-out mice to specifically delete STAT3 or gp130 in RPE, retina, or both RPE and retina. After intravitreal injection of LIF, we analyzed the expression levels of visual cycle genes and proteins, isomerase activity of RPE65, levels of rhodopsin protein, and the rates of dark adaptation and rhodopsin regeneration. We found that RPE65 protein levels and isomerase activity were reduced and recovery of bleachable rhodopsin was delayed in LIF-injected eyes. In mice with functional gp130/STAT3 signaling in the retina, rhodopsin protein was also reduced by LIF. However, the LIF-induced down-regulation of RPE65 required a functional gp130/STAT3 cascade intrinsic to RPE. Our data demonstrate that a single cytokine, LIF, can simultaneously and independently affect both RPE and photoreceptors through the same signaling cascade to reduce the generation and utilization of 11-*cis*-retinal.

The retinal pigment epithelium (RPE)[2] closely interacts with photoreceptors for the recycling of visual pigments and essential lipids and for the exchange of nutrients from the blood (1–3). Because of these essential interactions, disruptions in RPE function or viability result in retinal degenerations including Stargardt's disease, Best disease, and age-related macular degeneration (4–6). A major function of the RPE is the regeneration of 11-*cis*-RAL through a multistep enzymatic pathway known as the retinoid visual cycle (7–10). The central enzyme in the visual cycle, retinal pigment epithelium 65 (RPE65) protein, is expressed in the RPE and is the enzyme responsible for regeneration of photosensitive 11-*cis*-retinoid (9, 11). Excessive synthesis of 11-*cis*-RAL by the RPE is detrimental to photoreceptor health and survival (12, 13). In response to both light and mechanical stresses, visual cycle genes are down-regulated via a signal(s) originating from the retina, suggesting that this down-regulation is a general damage response of the RPE (14). Indeed, inhibition of RPE65 activity by retinoid and non-retinoid compounds is a promising pharmacological intervention for inherited retinal degenerations (15–17). Identifying endogenous pathways that can stimulate a natural down-regulation of RPE65 activity would not only address an interesting biological question, but the discovery could potentially be developed into a new therapeutic approach to prevent blindness.

We and others have shown that IL-6 family cytokines, including leukemia inhibitory factor (LIF) and ciliary neurotrophic factor (CNTF), are endogenously induced in response to light and inherited mutation-triggered stresses (18–25). These up-regulated cytokines protect the retina from degeneration through activation of the gp130 receptor and con-

* This work was supported, in whole or in part, by National Institutes of Health Grants R01EY16459 (to J. D. A.), R01EY012231 (to J. X. M.), R01EY018659 (to J. X. M.), R01EY019309 (to J. X. M.), R01EY019494 (to M. H. E.), EY012190 (NEI core grant), and Grants RR024215 and RR017703 (Center of Biomedical Research Excellence). This work was also supported by Foundation Fighting Blindness and an unrestricted grant from Research to Prevent Blindness, Inc.
[S] This article contains supplemental Figs. 1–7 and Tables 1 and 2.
[1] To whom correspondence should be addressed. Tel.: 352-273-8328; Fax: 352-273-7402; E-mail: jash@ufl.edu.

[2] The abbreviations used are: RPE, retinal pigment epithelium; LIF, leukemia inhibitory factor; CNTF, ciliary neurotrophic factor; 11-*cis*-RAL, 11-*cis*-retinal; LRAT, lecithin-retinol acyltransferase; MCT-1, monocarboxylate transporter-1; DKO, double knock-out mice; ERG, electroretinography.

sequent activation of STAT3 in the retina (26, 27). Studies have also shown that high levels of CNTF result in decreased mRNA and protein expression of phototransduction genes (28, 29), thus reducing the utilization of 11-*cis*-RAL in photoreceptor cells. To maintain health and balance in the production and utilization of retinoids, we predicted that LIF might also reduce the production of 11-*cis*-RAL in the RPE.

In this study we investigated whether STAT3 activation by LIF alters the activity of the visual cycle in RPE. We found that RPE65 mRNA, protein, and isomerase activity, bleachable rhodopsin content, and recovery of rod a-wave response after bleaching light are reduced in response to robust STAT3 activation. We used conditional knock-out mice for gp130 and STAT3 to demonstrate that the reduction in RPE65 required a functional gp130/STAT3 cascade in the RPE. Our results support the concept that endogenous stress responses in the retina can directly modulate the visual cycle in RPE cells and can control the rate of 11-*cis*-RAL production. The direct neuroprotective effects of LIF and CNTF coupled with the ability to down-regulate RPE65 activity suggest that gp130 agonists could provide a potent therapeutic strategy for retinal diseases that result from the toxic accumulation of retinoid byproducts.

EXPERIMENTAL PROCEDURES

Animals—All animal procedures were followed according to guidelines established by the ARVO (Association for Research in Vision and Ophthalmology) statement for the Use of Animals in Ophthalmic and Vision Research and were approved by Institutional Animal Care and Use Committees at the University of Oklahoma Health Sciences Center and the Dean A. McGee Eye Institute. *STAT3*$^{flox/flox}$ mice (30, 31) and *gp130*$^{flox/flox}$mice (32) were mated with *RPE-cre* mice (33) to generate conditional knock-out (KO) mice with RPE-specific deletion of STAT3 (*RPE-cre*$^{+}$; *STAT3*$^{flox/flox}$), referred to here as STAT3-RPE-cre KO, and gp130 (*RPE-cre*$^{+}$; *gp130*$^{flox/flox}$), referred to here as gp130-RPE-cre KO. In addition, *gp130*$^{flox/flox}$ were mated with *Chx10-cre*$^{+}$ mice (34), purchased from The Jackson Laboratory ((Chx10-EGFP/cre-,-ALPP)2Clc/J; #005105) to generate retina-specific conditional KO mice (*Chx10-cre*$^{+}$; *gp130*$^{flox/flox}$), referred to here as gp130-Ret-cre KO. Double KO mice with deletion of gp130 in both the retina and RPE were generated by mating gp130-Ret-cre KO by gp130-RPE-cre KO mice (*Chx10-cre*$^{+}$; *gp130*$^{flox/flox}$/*RPE-cre*$^{+}$; *gp130*$^{flox/flox}$), referred to here as gp130-Ret&RPE-cre DKO. Male Balb/cj mice were purchased from The Jackson Laboratory (#000651) and acclimated in our animal facility for 2 weeks before any experiments were performed. To ease the nomenclature in our studies with transgenic mice, we will refer to the floxed, not expressing cre littermate controls as wild type (WT) for each conditional KO strain. All mice used in this study were albino and homozygous for the L450 variant of RPE65 (12). All experiments were performed on 6–8-week-old albino mice unless otherwise stated. DNA was extracted from tail samples for genotyping. The sequences of primers used for genotyping are included in supplemental Table 1.

Intravitreal Injection—Recombinant human LIF was produced in our laboratory and injected intravitreally as described previously (35). Recombinant LIF was free of endotoxins, and purity was determined by LC/MS/MS. Briefly, a single dose of 0.25, 0.5, or 3.0 μg of LIF (1 μl total volume) was injected through the temporal limbus of one eye of anesthetized 6–8-week-old mice, whereas the same volume of PBS (vehicle) was injected in the other eye as a control. Eyes showing signs of damage, bleeding, or inflammation were excluded from analysis.

RNA Extraction and Quantitative Real-time PCR—Total RNA pooled from two eyecups containing retina, RPE, choroid, and sclera was extracted with TRI reagent (Sigma) 2 days after intravitreal injections of 3.0 μg of LIF in the right eye and PBS in the left eye. RNA was used for cDNA synthesis (iScript cDNA synthesis kit, Bio-Rad). The mRNA levels of selected visual cycle genes were measured using quantitative real-time PCR. Primers to RPE65, lecithin-retinol acyltransferase (LRAT), retinol dehydrogenase 5, interphotoreceptor retinoid-binding protein, and RPL19 (housekeeping gene) were designed using PrimerQuest software (Integrated DNA Technologies) spanning intron-exon boundaries to amplify the corresponding mRNAs without amplifying potentially contaminating genomic DNA (supplemental Table 2). Quantitative real-time PCR was carried out with the SYBR Green PCR master mix (Bio-Rad) using the MyiQ Single-Color Real-Time PCR detection system (Bio-Rad) following the manufacturer's instructions.

Western Blot—Eyecups (RPE+ choroid+ sclera) and retinas were harvested at the indicated time points after a single injection of LIF and homogenized in lysis buffer (50 mM Tris-HCl (pH 7.5), 150 mM NaCl, 2.0 mM EDTA, 1% (v/v) Nonidet P-40, 1 mM sodium orthovanadate, and protease inhibitor mixture (Calbiochem, #539131)). Protein content was measured using the BCA protein assay (Pierce, #23225) with bovine serum albumin as the standard.

Equal amounts of protein, tested to fit within the linear range of detection for the antibodies used (20, 10, or 1 μg for retinas and 7.5 μg for eyecups) were electrophoresed on 4–20% SDS-polyacrylamide gels (Invitrogen, #EC60285) and electroblotted to nitrocellulose membranes. Proteins were detected by Western blotting with the following primary antibodies: anti-rhodopsin (RET-P1, Abcam, Cambridge, MA #ab3267); anti-PDE6α (ABR, Golden, CO #PA1–720); anti-transducin α (Abcam, #ab74059); anti-RPE65 anti-LRAT, and anti-pSTAT3 to phosphorylated STAT3 (Cell Signaling Technology, Danvers, MA #9145L), anti-ezrin (Sigma, #E8897), anti-MCT1 (Millipore, Temecula, CA #AB3540P), and anti-β actin (Abcam, #ab6276) as loading control. For representative blots for rhodopsin, the numbers 1, 2, and 3 next to the protein bands depict monomers, dimers, and trimers of rhodopsin protein, respectively. For chemiluminescent detection, blots were incubated with HRP-conjugated secondary antibodies (Amersham Biosciences). Imaging of the blots and analysis of band intensities were performed by conventional image analysis using an Image Station 4000R and Kodak software (IS4000 R; v.4.5.1) A total of at least three mice per group were analyzed, and results from right (LIF-injected) and left (PBS control) eyes were compared.

Immunohistochemistry—STAT3 activation in the eyes of Balb/cj mice and in conditional KO and their control eyes (WT)

was assessed by immunohistochemistry at different time points after a single intravitreal injection of LIF. To stain sections, eyes were removed, and the cornea and lens were dissected away. The resulting eyecups were fixed for 20 min with 2% paraformaldehyde, 1× PBS supplemented with 1 mM sodium orthovanadate. Eyecups were cryoprotected by sequential incubations in PBS containing 10, 15, and 30% sucrose and then frozen in Optimal Cutting Temperature medium (Tissue-Tek, #4583). Retinal cryostat sections (14 μm) were rinsed with PBS containing 1% Triton X-100, blocked with 5% normal horse serum, and immunostained with anti-pSTAT3 antibody. Imaging was performed on an Olympus FluoView FV500 confocal laser scanning microscope (Olympus, Center Valley, PA, v.5.0). Imaging and microscope settings were identical for all samples. For experiments checking the efficiency of deletion of STAT3 or gp130, a total of four mice per group was analyzed, and data from right (LIF-injected) eyes were compared between KO and their WT control mice.

To measure phagocytic activity of RPE, gp130-Ret-cre KO and control mice were injected with 3.0 μg of LIF in one eye and PBS in the other eye as a control, and 5 days later their eyes were collected at 3 different time points: 7:30 a.m. (30 min after the lights go on in the animal facility), 9:00 a.m., and 3:00 p.m. Opsin-labeled phagosomes in the RPE were stained with anti-RET-P1 antibody and were counted on 5-μm-thick paraffin sections. Imaging was performed using Olympus FluoView FV500 confocal laser scanning microscope (Olympus, Center Valley, PA; v.5.0). Phagosome counting was performed using a Nikon Eclipse E800 epifluorescence microscope using the Meta View software (v7.1.1.0). A total of four eyes per group were analyzed, and data from right (LIF-injected) eyes were compared with left (PBS-injected) eyes. Phagosomes were counted in four equidistant regions along both superior and inferior retinal hemispheres to evaluate the center, mid-periphery, and periphery of each hemisphere. The values from each region were summed to give a total count for each eye (each region, 143 μm; the sum of total 8 regions was 1144 μm). Care was taken to use the same regions in each eye. Counts from four replicates were averaged for each group.

RPE65 Isomerase Activity—RPE65 enzymatic activity was assayed as described previously (36) with slight modifications. Mouse eyecup homogenates were prepared from Balb/cj mice that were not injected or 7 days after intravitreal injections with 3.0 μg LIF or PBS. The homogenates were incubated with 0.2 μM all-*trans*-[^{3}H]retinol in the presence of 25 μM cellular retinaldehyde-binding protein (CRALBP) in 10 mM 1,3-bis[tris(hydroxymethyl)methylamino]propane buffer (BTP), containing 0.1 M NaCl, 1% BSA (pH 8.0). This resulted in the formation of retinyl esters and 11-*cis*-retinol. After a 2-h incubation at 37 °C in the dark, the generated retinoids were extracted with methanol and hexane and analyzed by normal phase HPLC (for representative HPLC traces, see supplemental Fig. 7). The isomerase activity was expressed as 11-*cis*-retinol formed/2 h/mouse eye. Based on previous studies, we have found this assay to be linear over a wide range of time points (37).

Measurement of Rhodopsin Regeneration—To measure the effect of LIF on the rate of rhodopsin regeneration, gp130-Ret-cre KO mice were injected intravitreally with 3.0 μg of LIF in the right eye and with PBS in the left eye. Four days after injections, mice were dark-adapted overnight and then exposed to a period of photo-bleach consisting of diffuse, cool, white fluorescent light from the top of a cage (400 lux for 5 min). Immediately after the bleach (time = 0 min) a group of mice were killed, and their eyes were removed and snap-frozen. The remaining photobleached mice were returned to darkness, and their eyes were collected under dim red light at 10, 20, 30, and 60 min after the bleach. An additional group of mice were not exposed to photo-bleach and served as overnight dark-adapted controls.

Rhodopsin measurements were performed as described previously (38, 39) with slight modification. Briefly, under dim red light, each eye was homogenized in 100 μl of buffer containing 10 mM Tris-HCl (pH 7.4), 150 mM NaCl, 1 mM EDTA, 2% (w/v) octylglucoside, and 50 mM hydroxylamine. Homogenates were centrifuged at 16,000 × *g*, and soluble lysates were scanned from 270 to 800 nm in a spectrophotometer (Ultrospec 3000 UV-visible spectrophotometer, GE Healthcare). Samples were then bleached under room light for 10 min and scanned again. The difference spectra at 500 nm between pre- and post-bleached samples were used to determine rhodopsin content using a molar extinction coefficient of 42,000 M^{-1} (40). The values were normalized to the total lysate volume, and data are presented as rhodopsin content/eye. To determine the rhodopsin regeneration rate, the rhodopsin content was plotted *versus* dark adaptation time. The sigmoidal curve was fit to the Hill equation by nonlinear regression. The equation allowed for a determination of the total rhodopsin content/eye (B_{max}) and the time required to regenerate 50% of the total rhodopsin ($K_{0.5(rhodopsin)}$) after photobleach.

Electroretinography (ERG)—After overnight dark adaptation, mice were anesthetized with intraperitoneal injection of xylazine (7 mg/kg) and ketamine (40 mg/kg), and their pupils were dilated topically with 1% atropine sulfate and 10% phenylephrine. Anesthetized mice were kept on a heating pad at 37 °C throughout the recordings. A gold wire electrode was placed on the center of each cornea and overlaid with 1% methylcellulose. A platinum reference electrode was attached in the mouth, and a platinum needle electrode was attached to the tail to serve as ground. Full-field ERGs were recorded from both eyes using an Espion E2 ERG system with Colordome Ganzfeld dome (Diagnosys, Littleton, MA, v.4.0.51).

For full field scotopic ERG recordings, a series of increasing flash intensities (−2.7, −0.7, 0.3, 1.3, 2.3, and 2.6 log cd·s/m^2) was presented to mice after overnight dark adaptation (26). The amplitude of the rod a-wave was measured from base line to trough and the b-wave from a-wave trough to the b-wave peak. RPE-driven c-wave responses were elicited by a 2.6 log cd·s/m^2 intensity flash and recorded within a period of 15 s after the flash presentation.

To determine the effect of LIF on rod dark adaptation, we compared the recovery of rod ERG responses after photobleaching (16, 41, 42) in eyes injected with LIF (3 μg) to PBS-injected control eyes. Full field scotopic ERG responses were elicited in both eyes after overnight dark adaptation using a test flash of 2.3 log cd·s/m^2. This flash elicited the maximal rod photoreceptor a-wave response, as established by intensity *ver-*

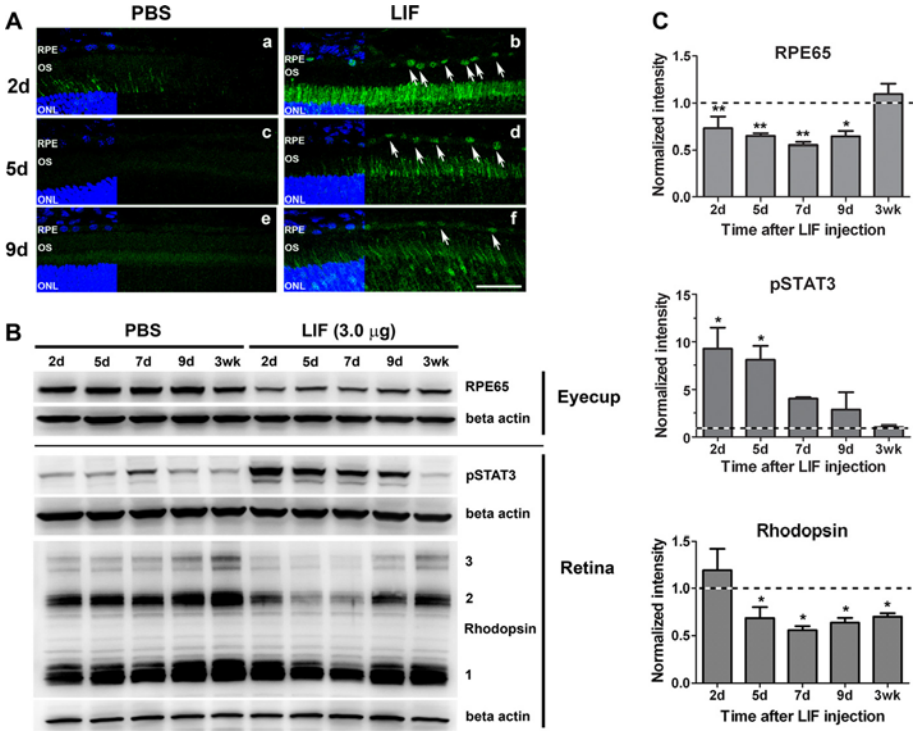

FIGURE 1. **LIF activates STAT3 and reduces expression of RPE65 protein in RPE and rhodopsin in the retina.** *A*, immunohistochemical detection of STAT3 phosphorylation (pSTAT3; *green*) on frozen sections from Balb/cj retinas revealed activation of STAT3 in RPE cell nuclei after a single intravitreal injection of 3.0 μg LIF (*white arrows* at 2 days (*b*), 5 days (*d*), or 9 days (*f*) after injection). Injection of PBS did not induce detectable STAT3 activation (*a*, *c*, and *e*). Nuclei were counterstained with DAPI (*blue*). *ONL*, outer nuclear layer; *OS*, outer segments. *Scale bar*, 50 μm. *B*, representative blots from eyecup and retina fractions show decreased RPE65 protein in the RPE fraction at various time points after intravitreal injection of 3.0 μg of LIF compared with PBS-treated controls. In the retinas of the same mice, LIF treatment induced increased activation of STAT3 and caused a time-dependent reduction in rhodopsin protein content. NOTE: *numbers 1*, *2*, and *3* labeled on the rhodopsin blot indicate rhodopsin monomer, dimer, and trimer, respectively. *C*, shown are densitometric analyses of RPE65 protein, STAT3 activation, and rhodopsin content at each time point after LIF injection. β-Actin was used as loading control. Normalizations were done to the respective PBS control. $n = 3$ for each group; * and ** $p < 0.05$ with respect to 3 weeks for RPE65; *, $p < 0.05$ with respect to 3 weeks for pSTAT3, and *, $p < 0.05$ with respect to 2 days for rhodopsin by one-way analysis of variance followed by Newman-Keuls post hoc test. *Error bars*, S.E.

sus response relationships. Mice were then exposed in the Ganzfeld dome to a steady field of white light at 2.3 log cd/m^2 for 5 min. At the end of the photobleach, the background illumination was turned off, and the same test flash of 2.3 log cd·s/m^2 was presented at time = 0 min and at 10-min intervals thereafter under fully dark conditions. For each eye, the a-wave response was normalized to the initial dark-adapted response (normalized Rm_{p3} amplitude).

Histological Analysis—After ERG recordings, mice were euthanized with CO_2, and the eyes were enucleated and marked with a green dye on the dorsal surface to mark the superior hemisphere. Eyes were then fixed in PERFIX (20% isopropyl alcohol, 2% trichloroacetic acid, 4% paraformaldehyde, and 2% zinc chloride) overnight and placed in 70% ethanol at room temperature for 2 days followed by embedding in paraffin. Sagittal sections through the center of the eye, including the optic disc, were cut at 5-μm thickness. Hematoxylin and eosin staining was performed to examine eye morphology.

Statistical Analysis—Statistical analyses were performed by using Graph pad Prism 5.0 software. The quantitative data are expressed as the mean ± S.E. for each group. The paired *t* test and unpaired *t* test were performed to assess the differences between the means. For multiple comparisons, one-way analysis of variance was performed along with the Newman-Keuls post hoc test.

RESULTS

LIF Activates STAT3 and Decreases the Levels of RPE65 in RPE—We previously showed that LIF, a member of the IL-6 family of cytokines, can protect photoreceptors under stress through gp130/STAT3 activation within photoreceptor cells (26, 35). In these studies we also observed that, in addition to activating signaling in the retina, LIF caused rapid and robust phosphorylation of STAT3 in RPE cells (35), suggesting that LIF may have an activity in RPE cells. In response to several retinal stresses, such as retinal detachment or bright light exposure, transcripts coding for visual cycle components, including RPE65, are down-regulated, suggesting the existence of a general RPE stress response capable of modulating visual cycle activity (14). In photoreceptors, IL6 family neurocytokines, such as CNTF (28, 29) and LIF (this study), can down-regulate the phototransduction machinery, which dramatically reduced the need for 11-*cis*-RAL in the retina. We hypothesized that LIF signaling in RPE cells may activate a parallel mechanism to down-regulate the visual cycle in RPE cells as part of a general protective response to reduce the accumulation of potentially toxic retinoid products. To test this hypothesis, we injected LIF intravitreally in the right eye and PBS in the left eye of Balb/cj mice and collected eyes at different time points for RNA, protein, and immunohistochemical analyses. STAT3 was robustly activated (pSTAT3; *green*) in RPE nuclei, and this activation

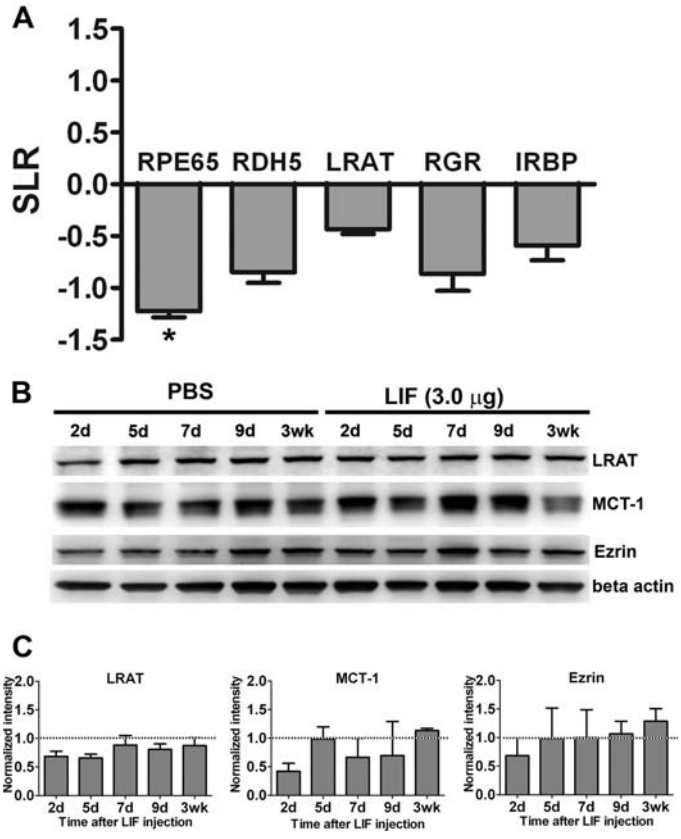

FIGURE 2. **LIF-induced down-regulation of RPE65.** *A*, quantitative real-time PCR analysis of visual cycle transcripts revealed that intravitreal injection of 3.0 μg of LIF significantly decreased the expression of RPE65 in comparison to PBS-injected eyes at 2 days post-injection. Gene expression was normalized to 60 S ribosomal protein L19 coding gene (RPL19) as housekeeping gene and compared with PBS; *SLR*, signal log ratio (1 unit of SLR = 2-fold of change; n = 3 for each group; *, $p < 0.05$ by paired t test. *Error bars*, S.E.). *B*, representative blots from eyecups show the protein contents of LRAT, MCT-1, and ezrin after intravitreal injections in Balb/cj mice. *C*, densitometric analysis of three independent experiments shows the analysis of protein contents of LRAT, MCT-1, and ezrin. β-Actin was used as loading control. Normalizations were done to the respective PBS control (n = 3 for each group. *Error bars*, S.E.

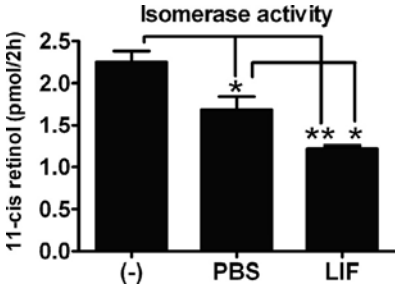

FIGURE 3. **LIF decreases the isomerase activity of RPE65.** The enzymatic activity of RPE65 was measured from eyecups of Balb/cj mice 7 days after a single injection of 3.0 μg of LIF or PBS. The isomerase activity was analyzed as the production of 11-*cis*-retinol after a 2-h incubation of Balb/cj mouse eyecup homogenates with the substrate all-*trans*-[^{3}H]retinol. Compared with uninjected (−) and PBS-injected eyecups, LIF-injected eyecups showed decreased isomerase activity of RPE65. n = 4 for each group; * and **, $p < 0.05$ by one-way analysis of variance followed by Newman-Keuls post hoc test. *Error bars*, S.E.

was persistent for up to 9 days after a single intravitreal injection of 3.0 μg LIF (Fig. 1*A*). Western blot analysis of protein lysates from RPE fractions (eyecup + choroid + sclera) showed that LIF significantly reduced the protein content of RPE65 relative to PBS-injected eyes (Fig. 1, *B* and *C*). The effect lasted more than 9 days, but RPE65 levels recovered by 3 weeks post-injection. Consistent with our previous reports (19, 26, 35), LIF also activated STAT3 in neuroretinas. LIF treatment also resulted in a reduction in rhodopsin protein levels (Fig. 1, *B* and *C*) as expected. Intravitreal injections of lower concentrations of LIF (0.25 and 0.5 μg) resulted in decreased RPE65 protein in the RPE fraction without reducing rhodopsin content in the neuroretina (supplemental Fig. 1), suggesting that RPE cells are more sensitive to LIF than photoreceptors in decreasing the expression of visual cycle components.

We measured the expression of RPE65, LRAT, retinol dehydrogenase 5, retinal G protein-coupled receptor, and interphotoreceptor retinoid-binding protein by quantitative real-time PCR. Our data showed that at 2 days post-injection, only RPE65 was down-regulated more than 2-fold and was statistically lower than control (Fig. 2*A*). By Western blot analysis, LRAT, monocarboxylate transporter-1 (MCT-1), and ezrin were not significantly reduced by LIF treatment (Fig. 2, *B* and *C*). These data suggest that the down-regulation of RPE65 was a specific effect triggered by LIF in RPE and affected both mRNA and protein levels.

LIF Reduces the Isomerase Activity of RPE65—The reduction in RPE65 protein suggested that LIF could reduce isomerase activity. To assess the functional activity of RPE65, we determined the generation of 11-*cis*- [^{3}H]retinol from all-*trans*-[^{3}H]retinol in Balb/cj eyecups collected 7 days after intravitreal injection of 3.0 μg of LIF and PBS. Consistent with the down-regulation of RPE65 mRNA and protein, intravitreal injection of LIF reduced the isomerase activity of RPE65 protein, in comparison to not injected and PBS-injected eyes (Fig. 3). In addition to the LIF-induced reduction of isomerase activity, we were surprised to observe a smaller reduction of isomerase activity in mice injected with PBS alone. Although we do not know the cause of this PBS effect, the reduced isomerase activity occurs without changing the level of RPE65 protein and without activating the gp130/STAT3 cascade. This suggests that there are additional mechanisms to regulate activity in response to mechanical injury.

Down-regulation of RPE65 Is Dependent on gp130/STAT3 in RPE—To determine whether the down-regulation of RPE65 was a direct effect of LIF activating the gp130/STAT3 pathway intrinsic to RPE cells or was caused by indirect signaling from photoreceptors, we used conditional knock-out mice with specific deletion of STAT3 (STAT3-RPE-cre KO) or gp130 (gp130-RPE-cre KO) in RPE cells. To assess the efficiency of STAT3 and gp130 deletion in RPE, we counted cells that were positive for pSTAT3 30 min after LIF injection (Fig. 4*A*). The immunohistochemical analysis demonstrated significant (~8-fold) reduction of LIF-induced STAT3 activation in both STAT3-RPE-cre KO and gp130-RPE-cre KO lines (Fig. 4*B*). The deletion was specific for the RPE as LIF activated STAT3 in the retinas of all mice but not in the RPE of the RPE conditional KO mice (supplemental Fig. 2). Loss of gp130 or STAT3 (data not shown) did not cause retinal degeneration or overt changes in retina or RPE structure or function (supplemental Fig. 3).

After establishing robust and specific deletion of gp130/STAT3 signaling in RPE, we next determined whether LIF

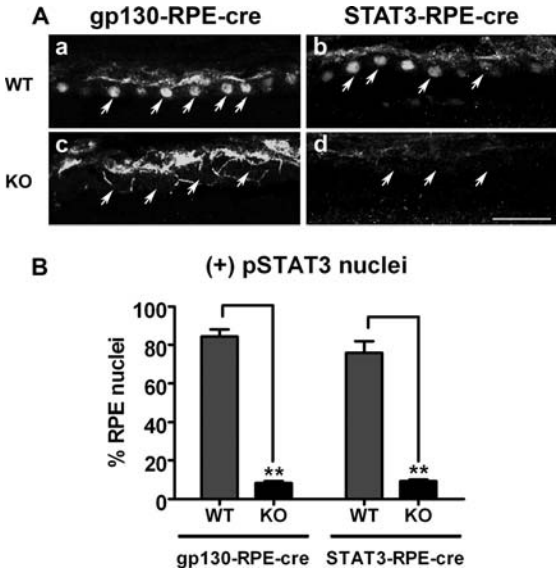

FIGURE 4. **Efficiency of deletion of gp130 and STAT3 in the gp130-RPE-cre KO and STAT3-RPE-cre KO mouse models.** *A*, shown is immunohistochemical detection of STAT3 activation (pSTAT3) on frozen retinal sections of gp130-RPE-cre littermates (gp130-RPE-cre WT *versus* gp130-RPE-cre KO, see *a* and *c*) and STAT3-RPE-cre littermates (STAT3-RPE-cre WT *versus* STAT3-RPE-cre KO, see *b* and *d*) 30 min after intravitreal injection with 0.5 μg LIF. *Scale bar*, 100 μm. *B*, shown is quantification of pSTAT3-positive nuclei staining in gp130-RPE-cre and STAT3-RPE-cre mouse systems, expressed as percentage of RPE nuclei 30 min after LIF injection. Compared with their respective WT controls, gp130-RPE-cre KO and STAT3-RPE-cre KO showed significantly reduced pSTAT3 staining specifically in RPE cells ($n = 4$ for each group, ** $p < 0.05$ by unpaired *t* test. *error bar*, S.E.).

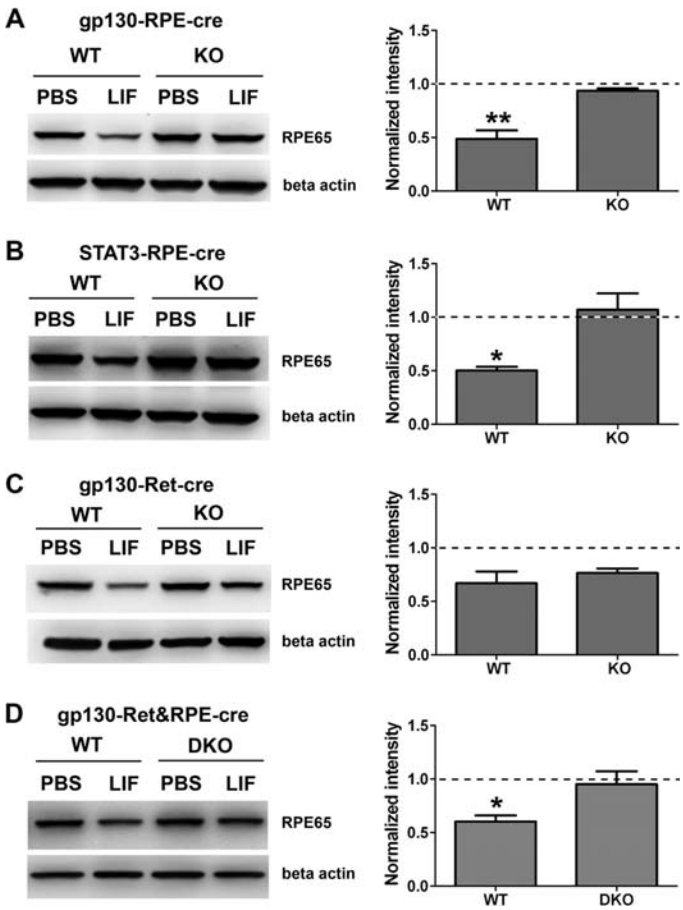

FIGURE 5. **The reduction of RPE65 protein levels is dependent on gp130/STAT3 signaling pathway in RPE cells.** Shown are representative blots (*left column*) and densitometric analysis of multiple blots (*right column*) of RPE65 protein content in eyecups 5 days after a single intravitreal injection of 3.0 μg of LIF. The values shown are the normalized signals of LIF-injected mice relative to the normalized signals of PBS controls (internal normalization for each sample to β-actin signal). The PBS controls are, therefore, set at the value of 1 (*dashed line*). The reduction of RPE65 protein level by LIF treatment seen in control mice was abolished in gp130-RPE-cre KO (*A*), STAT3-RPE-cre KO (*B*), and in gp130-Ret&RPE-cre DKO (*D*) eyecups. In the gp130-Ret-cre KO eyecups (retina only knock-out), LIF effectively reduced RPE65 at the same extent in both KO and WT (*C*). β-Actin was used as the loading control. $n =$ at least 3 for each group; *, $p < 0.05$ by unpaired *t* test comparing WT and KO. *Error bars*, S.E.

could still reduce RPE65 levels in the RPE. Western blot analysis showed that LIF injection did not decrease RPE65 levels in gp130-RPE-cre and STAT3-RPE-cre KO eyecups but was effective in reducing RPE65 in control (WT) littermates (Fig. 5, *A* and *B*). These results indicate that the gp130/STAT3 pathway intrinsic to RPE cells mediates the down-regulation of the visual cycle. In contrast, RPE65 protein was reduced in eyecups from LIF-injected mice lacking gp130 only in the retina (gp130-Ret-cre KO) (Fig. 5*C*). To confirm that gp130 in RPE is necessary for LIF-mediated reductions in RPE65, we generated double knock-out mice (DKO) mice lacking gp130 in both the retina and RPE. In these DKO mice LIF injection did not reduce RPE65 levels (Fig. 5*D*). These results demonstrate that LIF-induced signaling intrinsic to the RPE is necessary for LIF to induce reduction of RPE65.

In eyes injected with high doses of LIF (3 μg), we observed a coordinated decrease in the levels of both RPE65 and rhodopsin (Fig. 1*B*). We demonstrated that the LIF-induced down-regulation of RPE65 requires gp130/STAT3 signaling intrinsic to RPE (Fig. 5). To determine whether the LIF-induced reduction of rhodopsin was dependent on gp130/STAT3 signaling in the RPE, we injected LIF into eyes from mice with either gp130 or STAT3 deletion specific to RPE and measured rhodopsin protein by Western blotting. We found that deletion of gp130 or STAT3 in RPE did not reduce STAT3 activation in the retina nor the LIF-induced reduction of rhodopsin protein (Fig. 6, *A* and *B*). We then examined the effect of gp130 deletion in the retina on rhodopsin levels. The retina-specific gp130 deletion dramatically reduced STAT3 activation in the neuroretina (Fig. 6*C*) but did not affect the ability of LIF to activate STAT3 in the RPE (supplemental Fig. 4*A*). As shown in Fig. 6*C*, deletion of gp130 in the retina resulted in a loss of the ability of LIF to down-regulate rhodopsin protein. Not surprisingly, similar results were obtained for gp130-Ret&RPE-cre KO mice (Fig. 6*D*). In addition to rhodopsin, LIF induced down-regulation of additional phototransduction proteins, transducin-α and PDE6-α, in WT retinas but not in gp130-Ret&RPE-cre DKO retinas (supplemental Fig. 4*B*). Collectively, these data demonstrate that LIF-induced down-regulation of RPE65 in the RPE and rhodopsin in the retina is independent and due to intrinsic signaling within RPE and retina, respectively.

LIF Delays the Recovery of Rhodopsin after Photobleach—The data show that LIF could reduce RPE65 protein levels and isomerase activity in the RPE. We next wanted to determine whether the change in activity was sufficient to alter RPE support of photoreceptor function. We next determined whether we could measure reduced regeneration of 11-*cis*-RAL by RPE and whether this would translate into a delay in recovery of

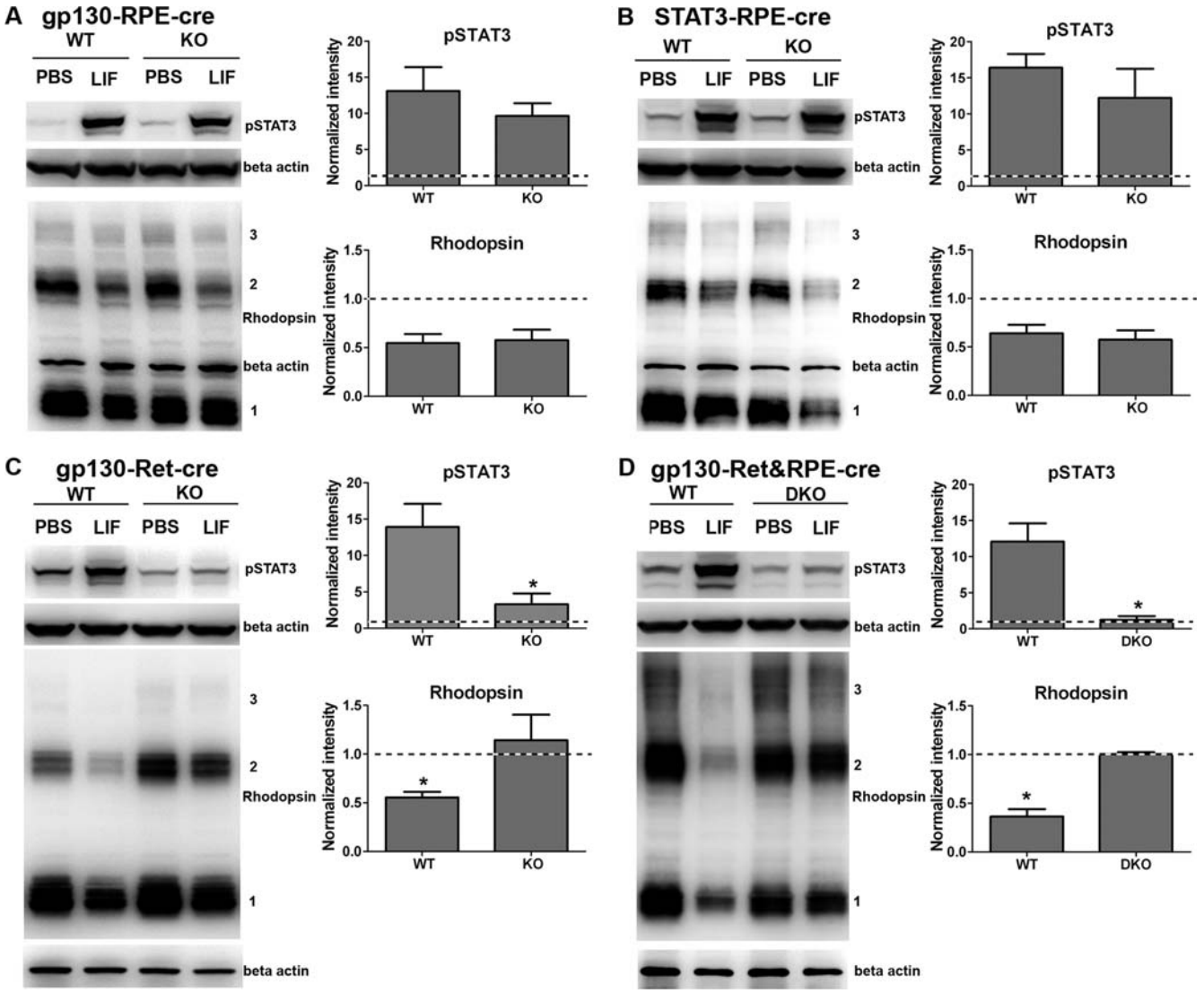

FIGURE 6. **LIF-mediated activation of retinal STAT3 and down-regulation of rhodopsin protein depends on gp130/STAT3 pathway within the neuroretina.** Shown are representative blots and analysis of multiple blots for pSTAT3 and rhodopsin protein content from retina homogenates 5 days after a single intravitreal injection of 3.0 μg LIF. In gp130-RPE-cre KO retinas (*A*) and STAT3-RPE-cre KO retinas (*B*), LIF induced activation of STAT3 and did not change rhodopsin protein levels compared with WT littermates. The deletion of retinal gp130 in gp130-Ret-cre KO mice (*C*) and in both retina and RPE in gp130-Ret&RPE-cre DKO (*D*) suppressed the activation of retinal STAT3 and the reduced levels of rhodopsin protein. β-Actin was used as the loading control. Normalizations were done to the respective PBS control and used for comparisons between WT and KO groups. n = at least 3 for each group; *, $p < 0.05$ by unpaired t test. *Error bars*, S.E.

rhodopsin after photobleach. To investigate this, we measured rhodopsin content spectrophotometrically at various time points after photobleach and compared rhodopsin recovery in LIF- and PBS-injected eyes. In the fully dark-adapted state, control WT mice had significantly reduced rhodopsin 5 days after LIF injection (Fig. 7, *A* and *B*). In contrast, deletion of gp130 in retina (Fig. 7*A*) or in retina and RPE (Fig. 7*B*) abolished the LIF-induced reduction in bleachable rhodopsin. This agrees with the Western blot data presented in Figs. 1 and 6. In contrast, total rhodopsin after complete dark adaptation was not reduced in gp130-Ret-cre KO mice, as photoreceptors lacked the LIF receptors. However, RPE cells could respond to LIF and had reduced RPE65 levels (see Fig. 5). In these mice we hypothesized that LIF would delay rhodopsin recovery if the reduction in RPE65 was biologically significant. Data show that the time to regenerate 50% of rhodopsin ($K_{0.5(\text{rhodopsin})}$) was delayed by more than 6 min in the LIF-injected eyes of gp130-Ret-cre KO mice compared with their paired PBS-injected eyes ($K_{0.5(\text{rhodopsin})} = 22.12 \pm 3.502$ min *versus* 15.56 ± 2.091 min; LIF *versus* PBS, respectively) (Fig. 7*C*). In contrast, in mice with gp130 deletion in both the retina and RPE (gp130-Ret&RPE-cre DKO), there was no difference in rhodopsin recovery ($K_{0.5(\text{rhodopsin})} = 14.25 \pm 4.476$ min *versus* 12.65 ± 4.476 min; LIF *versus* PBS, respectively) (Fig. 7*D*). LIF did not significantly change the total rhodopsin content/eye ($B_{\max}$) in the gp130-Ret-cre KO eyes ($B_{\max} = 345.8 \pm 40.78$ pmol/eye *versus* $B_{\max} = 315.0 \pm 28.4$ pmol/eye; LIF *versus* PBS, respectively) or in the gp130-Ret&RPE-cre KO eyes ($B_{\max} = 325.1 \pm 63.13$ pmol/eye *versus* $B_{\max} = 302.6 \pm 69.32$ pmol/eye; LIF *versus* PBS, respectively). Thus, the effect of LIF on rhodopsin recovery requires a functional gp130 receptor in RPE and the reduction of RPE65 was biologically significant on photoreceptor biochemistry.

To determine whether the 2-fold reduction in RPE65 could alter retina function, we measured the kinetics of rod dark

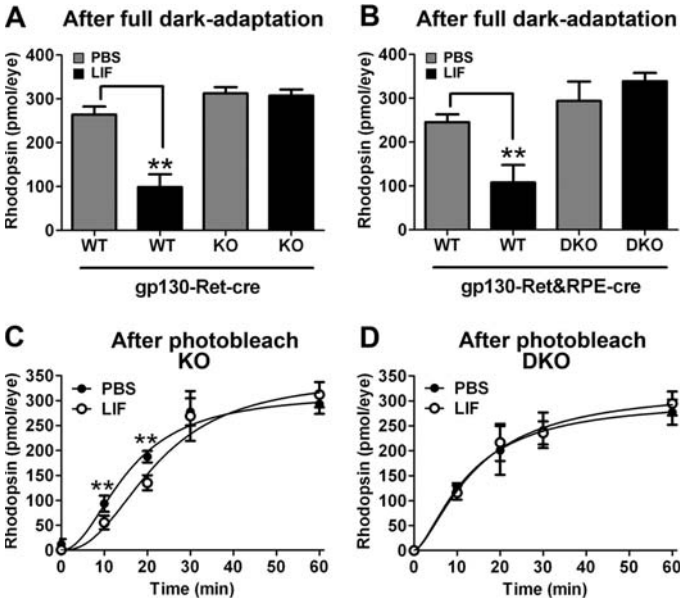

FIGURE 7. **LIF causes delayed recovery of bleachable rhodopsin through RPE-intrinsic gp130.** Shown are spectrophotometric determinations of bleachable rhodopsin in fully dark-adapted gp130-Ret-cre WT and gp130-Ret-cre KO eyes (*A*) and of gp130-Ret&RPE-cre WT and gp130-Ret&RPE-cre DKO eyes (*B*) 5 days after intravitreal 3.0-μg LIF or PBS injections. Total rhodopsin levels were reduced by LIF in WT mice but not in mice in which gp130 was deleted in the retina. n = at least 3 for each group; **, $p < 0.05$ comparing LIF- to PBS-injected eyes. *Error bars*, S.E. LIF significantly reduced rhodopsin recovery in mice in which gp130 was only deleted in the retina (*C*). However, rhodopsin recovery was unaffected by LIF in mice in which gp130 was also deleted in the RPE (*D*). n = at least 3 for each group; ** $p < 0.05$ comparing LIF- to PBS-injected eyes by paired *t* test. *Error bars*, S.E.

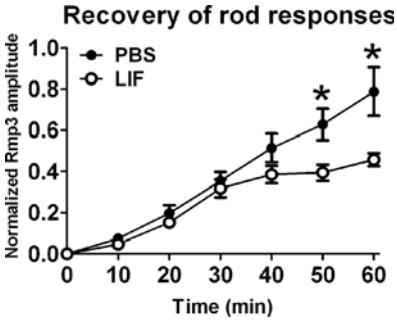

FIGURE 8. **The recovery of rod responses after photobleach is delayed in LIF-injected eyes.** Shown are electroretinographic recordings of the recovery of rod responses after a photobleach 5 days after a single intravitreal injection of PBS or 3.0 μg LIF. In gp130-Ret-cre KO mice, LIF caused a delay in dark adaptation with respect to PBS treatment. n = 10 for each group; *, $p < 0.05$ comparing PBS and LIF by paired *t* test. *Error bars*, S.E.

adaptation in LIF- and PBS-injected mice by ERG. We found that 5 days after a single LIF injection there was a significant delay in the recovery of rod responses after a photobleach (Fig. 8). The delay was observed at the longer time points and early time points, presumably because the rod a-wave amplitudes were small before 30 min of recovery. After this point, PBS-injected eyes continued to recover, but LIF-injected eyes were delayed. This result confirms that the reduction in RPE65 was sufficient to alter photoreceptor function.

LIF Does Not Alter Phagocytic Function of RPE—Because LIF can reduce the visual cycle, it was possible that LIF can reduce other functions of RPE. RPE cells are responsible for phagocytosing and digesting 10% of rod photoreceptor outer segments daily (43–46). This is an essential activity of RPE cells as impairment of phagocytosis results in the accumulation of a debris layer between photoreceptors and RPE and leads to retinal degeneration (47–49). To assess whether LIF causes significant changes in other RPE function, we performed assays to measure RPE phagocytic activity. We reasoned that because LIF can cause reduced rhodopsin content in photoreceptors, such an effect would confound the interpretation of phagocytic assays, as it would greatly affect the level of substrate available for phagocytosis in WT mice. Thus, we used the gp130-Ret-cre KO mice, in which the gp130 subunit is specifically deleted in the retina, whereas it is maintained in the RPE tissue. We collected eyes 5 days after PBS and LIF injection at different times of the day, 7:30 a.m. (half an hour after the lights are on in the animal facility), 9:00 a.m., and 3:00 p.m., and processed for immunohistochemistry. As expected, at 7:30 a.m., we observed a burst of phagocytosis that decreased throughout the day. This is a hallmark of circadian-regulated phagocytosis in RPE. This activity was identical in LIF- and PBS-injected eyes (supplemental Fig. 5). These data demonstrate that LIF stimulation down-regulated the visual cycle in RPE cells without altering another major function of RPE, such as phagocytosis. Further studies evaluating the effect of the LIF/gp130/STAT3 signaling cascade on other molecular events that might affect the activity of the visual cycle, such as the uptake of retinoids by the RPE from the choroidal blood, should be conducted to establish if this signaling cascade can trigger other mechanisms other than the down-regulation of RPE65 that can contribute to the down-regulation of the visual cycle.

DISCUSSION

Here we demonstrate a novel role for the gp130/STAT3 signaling pathway in RPE cells. Our data demonstrate that a single injection of LIF can decrease the isomerase activity in RPE cells *in vivo*. The decreased activity lasts for more than 9 days after a single high dose injection and is sufficient to reduce recovery from photobleach and extends dark adaptation time. Data also show that these effects require gp130 and STAT3 activation in RPE cells and involve reduced mRNA and protein expression of RPE65. The significance of these findings is that we have identified a paracrine factor that can coordinate activity in RPE and photoreceptors to reduce production and utilization of 11-*cis*-RAL. As we will discuss, this has important relevance to retinal degenerations.

Excessive accumulations of visual cycle byproducts such as A2E, photoisomers of A2E, and all-*trans*-RAL dimer conjugates are considered a primary cause of RPE atrophy in recessive Stargardt disease, a juvenile form of macular degeneration (50, 51), as well as in cone-rod dystrophy and atypical retinitis pigmentosa. In this context, limiting the activity of the RPE65 isomerase is a reasonable strategy to prevent such degenerations, and slowing the light-dependent cycling of retinoids activity has been suggested as a protection strategy (10, 12, 13). In fact, the use of compounds that slow down the renewal of the chromophore, 11-*cis*-RAL, has been indicated as a potential treatment for specific forms of retinal degeneration (16, 17, 52). Hypomorphic alleles of RPE65 such as the mouse M450 mutant have been shown to have about 40% of the normal isomerase

activity (53) and have been shown to have delayed dark adaptation (see Fig. 22 in Ref. 54). These studies show that a 50% reduction is biologically significant for the RPE visual cycle and is in very good agreement with the data presented in this study. Our study and these published studies show that a 40–50% reduction in RPE65 activity can affect vision. Also, this reduction is associated with protection because the M450 mutation is less sensitive to light damage and because these mice have slower degeneration in the presence of rhodopsin mutations (12, 13, 55). Our study suggests that agonists of the LIF/gp130/STAT3 pathway, which decrease RPE65 expression, may also have this therapeutic activity. Importantly, in response to both light damage and retinal detachment, down-regulation of RPE transcripts coding for visual cycle proteins is a generic endogenous response by the RPE (14). Our study suggests that down-regulation of the visual cycle in both the RPE and photoreceptors is coordinated by a single factor. This is the first report that identifies a specific factor that can explain this activity.

Intrinsic gp130 activation in photoreceptors is required to prevent the death of neurons in situations of acute light damage or genetic stress, suggesting that gp130 is essential to prevent or delay cell death in neurodegenerative diseases or chronic injury (19, 26, 27). Indeed, when gp130 ligands such as CNTF and LIF are provided exogenously, they protect photoreceptors from light damage (35, 56). In our previous report (35) we observed strong activation of STAT3 in the RPE after intravitreal injection of LIF, which prompted us to identify RPE functions that are modulated by STAT3.

Members of the STAT family of transcription factors, such as STAT1, STAT2, STAT5b, STAT6, and STAT3, were found in the adult RPE (57). In particular, phosphorylated STAT3 (pSTAT3) was localized to RPE nuclei and along with STAT5a was suggested as the most important modulator of RPE function. The activation of STAT3 was also reported in RPE cells coincident with the formation of scars in choroidal neovascular membranes of patients with age-related macular degeneration (58), indicating a possible role of STAT3 in the molecular responses of RPE cells to stress or disease. Recently, the expression of CNTF, cardiotrophin 1, oncostatin M, and LIF and the localization of their receptors were shown in primary cultures of human fetal RPE (59). In their work, treatment with CNTF and oncostatin M induced phosphorylation of STAT3 and increased RPE cell survival, supporting a role for the gp130/STAT3 pathway in modulating the polarized secretion of neurotrophic factors and cytokines from the apical side of the RPE to contribute to protection of photoreceptors.

Previous studies implicated IL-6 family members, such as CNTF (28, 29, 60), as negative regulators of the phototransduction cascade in photoreceptor cells. Here, we provide evidence that LIF robustly activates the gp130/STAT3 pathway in the RPE to down-regulate the visual cycle by decreasing the RNA (Fig. 2*A*), protein (Fig. 1, *B* and *C*), and enzymatic activity of RPE65 (Fig. 3). The effect was specific as the contents of other RPE proteins such as LRAT, MCT-1, and ezrin did not significantly differ between LIF-injected and the PBS-injected groups (Fig. 2, *B* and *C*). Furthermore, another major function of RPE, phagocytosis of the photoreceptor outer segments, was not influenced by LIF (supplemental Fig. 5).

In summary, we provide direct evidence for a novel role of the gp130/STAT3 pathway in RPE cells *in vivo*. In response to cytokines such as LIF, which are up-regulated by Müller cells in situations of retinal stress (22), the RPE can down-regulate the activity of the visual cycle by decreasing the expression and activity of the key component RPE65. Our findings describe a cell-autonomous phenomenon regulated by a unique pathway that can down-regulate the phototransduction cascade if expressed in retinal photoreceptors and can provide protection of photoreceptors under genetic- and light-triggered stresses. A complete understanding of the mechanism underlying this effect is of relevance for the application of cytokines such as LIF and CNTF in clinical trials for treatment of retinal neurodegenerative diseases.

REFERENCES

1. Bok, D. (1993) The retinal pigment epithelium. A versatile partner in vision. *J. Cell Sci. Suppl.* **17,** 189–195
2. Marmorstein, A. D. (2001) The polarity of the retinal pigment epithelium. *Traffic.* **2,** 867–872
3. Strauss, O. (2005) The retinal pigment epithelium in visual function. *Physiol. Rev.* **85,** 845–881
4. Franco, L. M., Zulliger, R., Wolf-Schnurrbusch, U. E., Katagiri, Y., Kaplan, H. J., Wolf, S., and Enzmann, V. (2009) Decreased visual function after patchy loss of retinal pigment epithelium induced by low dose sodium iodate. *Invest. Ophthalmol. Vis. Sci.* **50,** 4004–4010
5. Lopez, P. F., and Aaberg, T. M. (1992) Phenotypic similarities between Stargardt's flavimaculatus and pattern dystrophies. *Aust. N. Z. J. Ophthalmol.* **20,** 163–171
6. Zarbin, M. A. (1998) Age-related macular degeneration. review of pathogenesis. *Eur. J. Ophthalmol.* **8,** 199–206
7. Driessen, C. A., Winkens, H. J., Hoffmann, K., Kuhlmann, L. D., Janssen, B. P., Van Vugt, A. H., Van Hooser, J. P., Wieringa, B. E., Deutman, A. F., Palczewski, K., Ruether, K., and Janssen, J. J. (2000) Disruption of the 11-*cis*-retinol dehydrogenase gene leads to accumulation of *cis*-retinols and *cis*-retinyl esters. *Mol. Cell. Biol.* **20,** 4275–4287
8. Farjo, K. M., Moiseyev, G., Takahashi, Y., Crouch, R. K., and Ma, J. X. (2009) The 11-*cis*-retinol dehydrogenase activity of RDH10 and its interaction with visual cycle proteins. *Invest. Ophthalmol. Vis. Sci.* **50,** 5089–5097
9. Moiseyev, G., Chen, Y., Takahashi, Y., Wu, B. X., and Ma, J. X. (2005) RPE65 is the isomerohydrolase in the retinoid visual cycle. *Proc. Natl. Acad. Sci. U.S.A.* **102,** 12413–12418
10. Radu, R. A., Hu, J., Peng, J., Bok, D., Mata, N. L., and Travis, G. H. (2008) Retinal pigment epithelium-retinal G protein receptor-opsin mediates light-dependent translocation of all-*trans*-retinyl esters for synthesis of visual chromophore in retinal pigment epithelial cells. *J. Biol. Chem.* **283,** 19730–19738
11. Jin, M., Li, S., Moghrabi, W. N., Sun, H., and Travis, G. H. (2005) Rpe65 is the retinoid isomerase in bovine retinal pigment epithelium. *Cell* **122,** 449–459
12. Wenzel, A., Reme, C. E., Williams, T. P., Hafezi, F., and Grimm, C. (2001) The Rpe65 L450M variation increases retinal resistance against light-induced degeneration by slowing rhodopsin regeneration. *J. Neurosci.* **21,** 53–58
13. Wenzel, A., Grimm, C., Samardzija, M., and Remé, C. E. (2003) The genetic modifier Rpe65Leu(450). Effect on light damage susceptibility in c-Fos-deficient mice. *Invest. Ophthalmol. Vis. Sci.* **44,** 2798–2802
14. Rattner, A., Toulabi, L., Williams, J., Yu, H., and Nathans, J. (2008) The genomic response of the retinal pigment epithelium to light damage and retinal detachment. *J. Neurosci.* **28,** 9880–9889
15. Kubota, R., Boman, N. L., David, R., Mallikaarjun, S., Patil, S., and Birch, D. (2012) Safety and effect on rod function of ACU-4429, a novel small-molecule visual cycle modulator. *Retina* **32,** 183–188
16. Mandal, M. N., Moiseyev, G. P., Elliott, M. H., Kasus-Jacobi, A., Li, X.,

Chen, H., Zheng, L., Nikolaeva, O., Floyd, R. A., Ma, J. X., and Anderson, R. E. (2011) α-Phenyl-*N*-*tert*-butylnitrone (PBN) prevents light-induced degeneration of the retina by inhibiting RPE65 protein isomerohydrolase activity. *J. Biol. Chem.* **286,** 32491–32501
17. Travis, G. H., Golczak, M., Moise, A. R., and Palczewski, K. (2007) Diseases caused by defects in the visual cycle. Retinoids as potential therapeutic agents. *Annu. Rev. Pharmacol. Toxicol.* **47,** 469–512
18. Bürgi, S., Samardzija, M., and Grimm, C. (2009) Endogenous leukemia inhibitory factor protects photoreceptor cells against light-induced degeneration. *Mol. Vis.* **15,** 1631–1637
19. Chollangi, S., Wang, J., Martin, A., Quinn, J., and Ash, J. D. (2009) Preconditioning-induced protection from oxidative injury is mediated by leukemia inhibitory factor receptor (LIFR) and its ligands in the retina. *Neurobiol. Dis.* **34,** 535–544
20. Gao, H., and Hollyfield, J. G. (1995) Basic fibroblast growth factor in retinal development. Differential levels of bFGF expression and content in normal and retinal degeneration (rd) mutant mice. *Dev. Biol.* **169,** 168–184
21. Gao, H., and Hollyfield, J. G. (1996) Basic fibroblast growth factor. Increased gene expression in inherited and light-induced photoreceptor degeneration. *Exp. Eye Res.* **62,** 181–189
22. Joly, S., Lange, C., Thiersch, M., Samardzija, M., and Grimm, C. (2008) Leukemia inhibitory factor extends the lifespan of injured photoreceptors *in vivo*. *J. Neurosci.* **28,** 13765–13774
23. Liu, C., Peng, M., Laties, A. M., and Wen, R. (1998) Preconditioning with bright light evokes a protective response against light damage in the rat retina. *J. Neurosci.* **18,** 1337–1344
24. Wen, R., Song, Y., Cheng, T., Matthes, M. T., Yasumura, D., LaVail, M. M., and Steinberg, R. H. (1995) Injury-induced up-regulation of bFGF and CNTF mRNAS in the rat retina. *J. Neurosci.* **15,** 7377–7385
25. Yu, D. Y., Cringle, S., Valter, K., Walsh, N., Lee, D., and Stone, J. (2004) Photoreceptor death, trophic factor expression, retinal oxygen status, and photoreceptor function in the P23H rat. *Invest. Ophthalmol. Vis. Sci.* **45,** 2013–2019
26. Ueki, Y., Le, Y. Z., Chollangi, S., Muller, W., and Ash, J. D. (2009) Preconditioning-induced protection of photoreceptors requires activation of the signal-transducing receptor gp130 in photoreceptors. *Proc. Natl. Acad. Sci. U.S.A.* **106,** 21389–21394
27. Ueki, Y., Chollangi, S., Le, Y. Z., and Ash, J. D. (2010) gp130 activation in Müller cells is not essential for photoreceptor protection from light damage. *Adv. Exp. Med. Biol.* **664,** 655–661
28. Wen, R., Song, Y., Kjellstrom, S., Tanikawa, A., Liu, Y., Li, Y., Zhao, L., Bush, R. A., Laties, A. M., and Sieving, P. A. (2006) Regulation of rod phototransduction machinery by ciliary neurotrophic factor. *J. Neurosci.* **26,** 13523–13530
29. Wen, R., Song, Y., Liu, Y., Li, Y., Zhao, L., and Laties, A. M. (2008) CNTF negatively regulates the phototransduction machinery in rod photoreceptors. Implication for light-induced photostasis plasticity. *Adv. Exp. Med. Biol.* **613,** 407–413
30. Akira, S. (2000) Roles of STAT3 defined by tissue-specific gene targeting. *Oncogene* **19,** 2607–2611
31. Takeda, K., Noguchi, K., Shi, W., Tanaka, T., Matsumoto, M., Yoshida, N., Kishimoto, T., and Akira, S. (1997) Targeted disruption of the mouse Stat3 gene leads to early embryonic lethality. *Proc. Natl. Acad. Sci. U.S.A.* **94,** 3801–3804
32. Betz, U. A., Bloch, W., van den Broek, M., Yoshida, K., Taga, T., Kishimoto, T., Addicks, K., Rajewsky, K., and Müller, W. (1998) Postnatally induced inactivation of gp130 in mice results in neurological, cardiac, hematopoietic, immunological, hepatic, and pulmonary defects. *J. Exp. Med.* **188,** 1955–1965
33. Le, Y. Z., Zheng, W., Rao, P. C., Zheng, L., Anderson, R. E., Esumi, N., Zack, D. J., and Zhu, M. (2008) Inducible expression of cre recombinase in the retinal pigmented epithelium. *Invest. Ophthalmol. Vis. Sci.* **49,** 1248–1253
34. Rowan, S., and Cepko, C. L. (2004) Genetic analysis of the homeodomain transcription factor Chx10 in the retina using a novel multifunctional BAC transgenic mouse reporter. *Dev. Biol.* **271,** 388–402
35. Ueki, Y., Wang, J., Chollangi, S., and Ash, J. D. (2008) STAT3 activation in photoreceptors by leukemia inhibitory factor is associated with protection from light damage. *J. Neurochem.* **105,** 784–796
36. Moiseyev, G., Crouch, R. K., Goletz, P., Oatis, J., Jr., Redmond, T. M., and Ma, J. X. (2003) Retinyl esters are the substrate for isomerohydrolase. *Biochemistry* **42,** 2229–2238
37. Moiseyev, G., Takahashi, Y., Chen, Y., Kim, S., and Ma, J. X. (2008) RPE65 from cone-dominant chicken is a more efficient isomerohydrolase compared with that from rod-dominant species. *J. Biol. Chem.* **283,** 8110–8117
38. Ranchon, I., LaVail, M. M., Kotake, Y., and Anderson, R. E. (2003) Free radical trap phenyl-*N*-*tert*-butylnitrone protects against light damage but does not rescue P23H and S334ter rhodopsin transgenic rats from inherited retinal degeneration. *J. Neurosci.* **23,** 6050–6057
39. Tanito, M., Brush, R. S., Elliott, M. H., Wicker, L. D., Henry, K. R., and Anderson, R. E. (2009) High levels of retinal membrane docosahexaenoic acid increase susceptibility to stress-induced degeneration. *J. Lipid Res.* **50,** 807–819
40. Irreverre, F., Stone, A. L., Shichi, H., and Lewis, M. S. (1969) Biochemistry of visual pigments. I. Purification and properties of bovine rhodopsin. *J. Biol. Chem.* **244,** 529–536
41. Mata, N. L., Tzekov, R. T., Liu, X., Weng, J., Birch, D. G., and Travis, G. H. (2001) Delayed dark-adaptation and lipofuscin accumulation in abcr$^{+/-}$ mice. Implications for involvement of ABCR in age-related macular degeneration. *Invest. Ophthalmol. Vis. Sci.* **42,** 1685–1690
42. Weng, J., Mata, N. L., Azarian, S. M., Tzekov, R. T., Birch, D. G., and Travis, G. H. (1999) Insights into the function of Rim protein in photoreceptors and etiology of Stargardt's disease from the phenotype in abcr knockout mice. *Cell* **98,** 13–23
43. Bosch, E., Horwitz, J., and Bok, D. (1993) Phagocytosis of outer segments by retinal pigment epithelium. Phagosome-lysosome interaction. *J. Histochem. Cytochem.* **41,** 253–263
44. LaVail, M. M. (1976) Rod outer segment disc shedding in relation to cyclic lighting. *Exp. Eye Res.* **23,** 277–280
45. LaVail, M. M. (1980) Circadian nature of rod outer segment disc shedding in the rat. *Invest. Ophthalmol. Vis. Sci.* **19,** 407–411
46. Nandrot, E. F., Anand, M., Almeida, D., Atabai, K., Sheppard, D., and Finnemann, S. C. (2007) Essential role for MFG-E8 as ligand for αvβ5 integrin in diurnal retinal phagocytosis. *Proc. Natl. Acad. Sci. U.S.A.* **104,** 12005–12010
47. Bok, D., and Hall, M. O. (1971) The role of the pigment epithelium in the etiology of inherited retinal dystrophy in the rat. *J. Cell Biol.* **49,** 664–682
48. Chaitin, M. H., and Hall, M. O. (1983) Defective ingestion of rod outer segments by cultured dystrophic rat pigment epithelial cells. *Invest. Ophthalmol. Vis. Sci.* **24,** 812–820
49. Strick, D. J., Feng, W., and Vollrath, D. (2009) Mertk drives myosin II redistribution during retinal pigment epithelial phagocytosis. *Invest. Ophthalmol. Vis. Sci.* **50,** 2427–2435
50. Radu, R. A., Hu, J., Yuan, Q., Welch, D. L., Makshanoff, J., Lloyd, M., McMullen, S., Travis, G. H., and Bok, D. (2011) Complement system dysregulation and inflammation in the retinal pigment epithelium of a mouse model for Stargardt macular degeneration. *J. Biol. Chem.* **286,** 18593–18601
51. Sparrow, J. R., Fishkin, N., Zhou, J., Cai, B., Jang, Y. P., Krane, S., Itagaki, Y., and Nakanishi, K. (2003) A2E, a byproduct of the visual cycle. *Vision Res.* **43,** 2983–2990
52. Golczak, M., Maeda, A., Bereta, G., Maeda, T., Kiser, P. D., Hunzelmann, S., von Lintig, J., Blaner, W. S., and Palczewski, K. (2008) Metabolic basis of visual cycle inhibition by retinoid and nonretinoid compounds in the vertebrate retina. *J. Biol. Chem.* **283,** 9543–9554
53. Redmond, T. M., Weber, C. H., Poliakov, E., Yu, S., and Gentleman, S. (2007) Effect of Leu/Met variation at residue 450 on isomerase activity and protein expression of RPE65 and its modulation by variation at other residues. *Mol. Vis.* **13,** 1813–1821
54. Lamb, T. D., and Pugh, E. N., Jr. (2004) Dark adaptation and the retinoid cycle of vision. *Prog. Retin. Eye Res.* **23,** 307–380
55. Samardzija, M., Wenzel, A., Naash, M., Remé, C. E., and Grimm, C. (2006) Rpe65 as a modifier gene for inherited retinal degeneration. *Eur. J. Neurosci.* **23,** 1028–1034
56. LaVail, M. M., Unoki, K., Yasumura, D., Matthes, M. T., Yancopoulos,

G. D., and Steinberg, R. H. (1992) Multiple growth factors, cytokines, and neurotrophins rescue photoreceptors from the damaging effects of constant light. *Proc. Natl. Acad. Sci. U.S.A.* **89,** 11249–11253
57. Zhang, S. S., Wei, J. Y., Li, C., Barnstable, C. J., and Fu, X. Y. (2003) Expression and activation of STAT proteins during mouse retina development. *Exp. Eye Res.* **76,** 421–431
58. Fasler-Kan, E., Wunderlich, K., Hildebrand, P., Flammer, J., and Meyer, P. (2005) Activated STAT 3 in choroidal neovascular membranes of patients with age-related macular degeneration. *Ophthalmologica* **219,** 214–221
59. Li, R., Wen, R., Banzon, T., Maminishkis, A., and Miller, S. S. (2011) CNTF mediates neurotrophic factor secretion and fluid absorption in human retinal pigment epithelium. *PLoS One* **6,** e23148
60. Rhee, K. D., Ruiz, A., Duncan, J. L., Hauswirth, W. W., Lavail, M. M., Bok, D., and Yang, X. J. (2007) Molecular and cellular alterations induced by sustained expression of ciliary neurotrophic factor in a mouse model of retinitis pigmentosa. *Invest. Ophthalmol. Vis. Sci.* **48,** 1389–1400